International Transaction Journal of Engineering, Management, & Applied Sciences & Technologies

http://TuEngr.com

PAPER ID: 10A15A

AN INVESTIGATION OF WIDEBAND MIMO CHANNEL CHARACTERISTICS IN RECTANGULAR TUNNEL

Asad Saleem [a,c*], Sherazi Syed Nisar Yousaf [b*]

[a] *Key Laboratory of Specialty Fiber Optics and Optical Access Networks, Joint International Research Laboratory of Specialty Fiber Optics and Advanced Communication, Shanghai Institute for Advanced Communication and Data Science, Shanghai University, 200444, Shanghai, CHINA.*

[b] *School of Communication and Information Engineering, Taiyuan University of Technology, 030100, Shanxi Province, CHINA.*

[c] *Shenzhen Key Laboratory of Antennas and Propagation, College of Electronics and Information Engineering, Shenzhen University, 518060, Shenzhen, CHINA.*

ARTICLEINFO

Article history:
Received 20 May 2019
Received in revised form 09 August 2019
Accepted 19 August 2019
Available online 26 August 2019

Keywords:
Leaky coaxial cable (LCX); Delay spread; Long term evolution for metro (LTE-M); Power delay profile (PDP); SISO; NLOS; LOS; Wireless Insite (WISE); RMS-DS.

ABSTRACT

In this paper, the power delay profile (PDP) and root mean square delay spread (RMS-DS) relationship is demonstrated to satisfy the LTE-M criteria for rectangular tunnel area at 1.8GHz. The leaky coaxial cable (LCX) was exploited as a transmitting antenna for both single-input single-output (SISO) and multi-input multiple-output (MIMO) systems. The effect of changing the received antenna (Rx) distance on the variation of received power using the Ray-Tracing Method is investigated. The reflected (NLOS) and line of sight (LOS) paths between the LCX and receiving antenna for both vertical and horizontal polarizations are deliberated and it was found that the horizontal polarized LCXs accomplish better performance than the vertically polarized cables used for both SISO and MIMO systems under tunnel environment. Furthermore, it was determined that the minimum distance between transmitting and receiving antennas can acquire higher received power.

1. INTRODUCTION

Long-Term Evolution for the metro (LTE-M) technique is recognized as a firm communications tactic for the future city rail transit systems because of a small number of shortcomings of wireless local area networks (WLAN) in the communication-based train control (CBTC) structure. The key consequences of LTE-M structures are better data rates and higher spectral efficiency based communications. In order to provide long term and steady communications, LTE-M mostly uses LCX for indoor environments such as tunnels, malls, subways, etc (Nakamura et al., 1996; Schwarz & Rupp, 2016). In small areas when the conventional antenna system is used, the attenuation of

*Corresponding author (A.Saleem, S.S.N. Yousaf). E-mail: asadalvi64@yahoo.com, shah.nisar@hotmail.com

radiated waves' gets severe after many times of scattering and reflection. The radiation characteristics and antenna parameters have substantial effects on the field coverage (Li & Wang, 2016). LCX has been used for many decades due to its massive advantages under indoor environments over orthodox antenna such as easy installation, confirming limited interference between the cells, and steady coverage (Wang et al., 2016). LCXs have principally consistent linearly slotted arrays having static-phases delay between two adjacent slots, moreover the periodic slots are slash in vast metallic planes having slight impact on scattered field (Wang et al., 2012).

Radio communications in the underground area rely on the environmental circumstance nearby the LCX, neighboring electromagnetic field intensity (EMI) and installation arrangement of LCX (Zhao et al., 2008). Ray Tracing (RT) methodology is widely applied for a meticulous approximation of the radio channels limitations and substantial accuracy of the neighboring field estimation for indoor atmosphere. The proper modification of the slots period of LCXs and configuration w.r.t the receiving antenna (Rx) can reduce the uncertainties of field. Ray-based transmission analysis such as multiplication to diffused scattering, multi-dimensional radio channel characterization, MIMO capacity assessments is deliberated in Fuschini et al. (2015). In underground tunnel situation, the physical wall material properties have vital impact on the electromagnetic features. The coupling losses (CL) of LCXs decrease under the condition where the dielectric coefficient of some material of the sidewall or roof gets higher or the operating frequency rises (Kim & Eom, 2007). Normally, single LCX is utilized as single transmitting antenna w.r.t single receiver antenna (SISO). Therefore in order to achieve higher performance, more than single LCX is lined up to design the MIMO system. In Emami et al. (2016), the two different LCXs were used to propose 2x2 underground corridor scenarios and office landscape based MIMO system. The experimental and theoretical results by Medbo & Nilsson (2012) reveal that LCX is appropriate for the MIMO channel in underground or tunnel environment. Furthermore, (Medbo & Nilsson, 2012) also disclose that the quality of MIMO channel gets poorer from the i.i.d channel when the LCXs were separated much closer.

In Ruisi et al. (2011), the three-dimensional (3D) frequency transfer function (FTF) was acquired based on an experimental campaign conducted in three different zones and power delay profiles (PDPs) were estimated. The PDPs in the line of sight (LoS) path meets very well to the exponential distribution. Due to the increment of measuring distance for the indoor tunnel, the line of sight component vanishes and several reflections stay because of the obscuration in tunnel. The root-mean-square delay spread (RMS-DS) is very important parameter that is widely used to describe the time-based dispersive attributions of multipath MIMO channels. As a matter of fact, the existence of obstacles in tunnel atmosphere has unpredictable special effects at the multipath channel (Shuang-de et al., 2017; Collonge et al., 2003). Moreover for radio channels, the RMS-DS rises when scattering and reflections induce greater transmission delay times. In Liao et al. (2013), a 3D image technique was presented to calculate the wireless local area network (WLAN) channel impulse response (CIR) for many locations of receiving antenna. Based on the CIR, the RMS-DS and the number of multipath components were computed. It was found that the RMS-DS for arched straight corridor was smaller than all other corridors regardless of their shapes. However, the previous studies deliver numerous results but most of these studies have insufficiency of real-time experiments in tunnel environment.

In this paper, the PDP and RMS-DS are explained thoroughly in the rectangular tunnel atmosphere at the 1.8GHz frequency. The RT approach was applied to explore the LCXs positioning impact on the SISO and MIMO channel characteristics. The horizontal and vertical polarized LCXs are under consideration. The paper is arranged as follows. Section II discusses the channel modeling. The methodology of PDP and RMS-DS estimation is given in Section III. Section IV deals with the simulated results and discussions of SISO and MIMO channels by considering both horizontal and vertical polarized LCXs and section V demonstrates the conclusion.

2. CHANNEL MODELING

The radiated field gives a brief introduction related to transfer of the energy/power from any source to the absolute destination in some specific pattern of the electric rays. The electric field complies the distance law of Inverse Square to some particular source. LCXs have periodic slots on the outermost conducting layer which facilitates the waves to radiate from the surface. Lately, various kinds of periodic slots of LCXs are fabricated based on the environmental condition and desires of users but in this work we deal with only vertical and horizontal polarized LCXs. Horizontal polarized LCXs slots are configured horizontal to propagation direction of LCX, and inverse case is considered for vertical polarized LCX (Zhang et al.,2006).The field from the circumferentially polarized LCX is estimated as follows

$$E_{\varphi} = V(\theta,\varphi)\frac{e^{-jk_0 r}}{r} sin\theta \quad (1),$$

where $V(\theta,\varphi) = \frac{jVcos\theta}{\pi^2\, bk_0 sin^3\theta}\sum_{n=-5}^{n=+5}\frac{ne^{jn\varphi}j^{n+1}}{H_n^{(2)'}(bk_0 sin\theta)} \times \frac{sinn\alpha}{n} - \frac{m\, sinm\alpha\, cosn\alpha - ncosm\alpha\, sinn\alpha}{(m^2-n^2)\cos m\alpha}$ with $m = k_0 b$. E_z stays constant alongside z-axis due to the very smaller width w of the slot, p is the period of the slot, $H_n^{(2)'}$ is the Hankel function of n^{th}ranked, φ is angle amongst x-axis and r', and θ is angle amongst z-axis and r. The distance from origin o to some location in space is r and it has the projection r' in xoy plane as shown in Figure. 1. The vertically polarized portion of E_{φ} can be calculated by introducing the Ray-Tracing method.

$$E_y = V(\theta_i,\varphi_i)\frac{e^{-jk_0\ (r_i+r_{i1})-\ j\beta_i P}}{r_i+r_{i1}}\ sin\theta_i\ cos\varphi_i\ \Gamma_h \quad (2),$$

where $r_i = \sqrt{{x_o}^2+{y_0}^2+{z_0}^2}$, $r_{i1} = \sqrt{{x_0}^2+(h-h_0)^2+(ip-z_0)^2}$

$\varphi_i = arccos\ (\frac{x_0}{\sqrt{{x_0}^2+{h_0}^2}})$; $\theta_i = arctan\ (\frac{\sqrt{{x_0}^2+{h_0}^2}}{z_0})$

$\beta = k_0\sqrt{\epsilon_r}$; $\gamma = \arctan(\frac{x_0}{\sqrt{{z_0}^2+{h_0}^2}})$.

The term Γ_h is reflection coefficients of horizontally polarized rays, z_0 is residual distance initiating from existing slot to the remaining z-axis, where h_o are perpendicular distance amongst the incident point and cable, x_o is the horizontal distance among the cable and the left-hand metope of space, and finally $(\epsilon_1 - j\epsilon_1')$ is the dielectric coefficient along the tunnel walls. The vertical

*Corresponding author (A.Saleem, S.S.N. Yousaf). E-mail: asadalvi64@yahoo.com, shah.nisar@hotmail.com Transaction Journal of Engineering, Management, & Applied Sciences & Technologies. Volume 10 No.15 ISSN 2228-9860 eISSN 1906-9642 CODEN: ITJEA8 Paper ID:10A15A http://TUENGR.COM/V10A/10A15A.pdf DOI: 10.14456/ITJEMAST.2019.195

polarized wave's reflection coefficients are calculated:

$$\Gamma_v = \frac{(\epsilon_1 - j\epsilon_1')sin\gamma - \sqrt{(\epsilon_1 - j\epsilon_1') - cos^2\gamma}}{(\epsilon_1 - j\epsilon_1')sin\gamma + \sqrt{(\epsilon_1 - j\epsilon_1') - cos^2\gamma}} \quad (3)$$

The horizontal polarized wave's reflection coefficients are written as

$$\Gamma_h = \frac{sin\gamma - \sqrt{(\epsilon_1 - j\epsilon_1') - cos^2\gamma}}{sin\gamma + \sqrt{(\epsilon_1 - j\epsilon_1') - cos^2\gamma}} \quad (4)$$

The total field is assessed by adding the effects of all other slots of LCX:

$$E_{y\Sigma} = \sum_{i=1}^{N} V(\theta_i, \varphi_i) \frac{e^{-jk_0(r_i + r_{i1}) - j\beta_i P}}{r_i + r_{i1}} sin\theta_i \, cos\varphi_i \Gamma_v \quad (5)$$

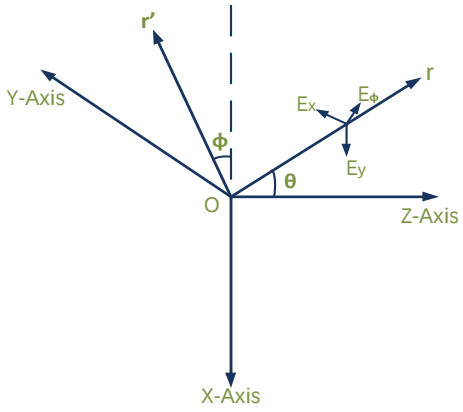

Figure 1: The radiated field pattern of LCX

3. ENERGY CONSERVATION

The geometry of the surrounding area, i.e., structure, density and the size of the building's cars, trees, etc., effects the propagation through the wireless channel. The conservation of energy indicates that the energy density integral for every closed surface nearby the transmitters (Tx) should be equivalent to transmitting power. Assuming that there exists a closed surface that follows a spherical shape with a radius d and having a transmitter at its center, and assuming that the transmitting antenna is isotropic, the energy density of the surface is $P_{Tx}/\left(4\pi d^2\right)$. The "effective area" of the receiving antenna is expressed as A_{Rx}. We can assume that the energy that is incident onto the area is received by the receiving antenna so that the energy that will be received is given as (Fontan & Espieira, 2008)

$$P_{Rx}(d) = P_{Tx} \frac{1}{4\pi d^2} A_{Rx} \quad (6)$$

If the transmitting antenna is not isotropic, the power density required to multiplied by antenna gain in the direction of Rx, which is assumed as

$$P_{Rx}(d) = P_{Tx} G_{Tx} \frac{1}{4\pi d^2} A_{Rx} \quad (7)$$

The product of the power of the transmitting antenna and the desired directional gain is known as the corresponding isotropic radiant energy (Equivalent Isotropically Radiated Power, EIRP). For

a given power density, the effective antenna area is proportional to the power received from the antenna connection. It can be proved that the effective area of the antenna has a simple relation with the antenna gain:

$$G_{Rx} = \frac{4\pi}{\lambda^2} A_{Rx} \tag{8}$$

Among them is the carrier wavelength, the formula (3.3) is brought into (3.2), and the receiving energy is obtained from the function with a transceiver distance d in the form of the variable, also known as the Friis Law:

$$P_{Rx}(d) = P_{Tx} G_{Tx} G_{Rx} \left(\frac{\lambda}{4\pi d} \right)^2 \tag{9}.$$

Friis's law points out that attenuation in free space increases with frequency.

3.1 POWER DELAY PROFILE

The PDP directs the received power of signal against the time delay, i.e., through indicating the relative extent of receiving power at the Rx antenna during the time duration of $(\tau, \tau + d\tau)$ (Molisch, 2006; Cui & Tellambura, 2006). In several communications systems, such as the OFDM, sub-channels and noise variance, PDPs are required for frequency offset valuations and channel approximation (Cui & Tellambura, 2005). Owing to the significance of PDP, many experimental performances have been established for it, including for different outdoor and indoor and vehicle to vehicle channels.

In the research of wireless channels, channel pulse response can be considered as a generalized stationary stochastic process in any short time. Because the channel studied in this paper is a quasi-static channel, the average power delay spectrum (PDP) can be achieved directly through the squares of the amplitude of N impulse response in time mean (Cox & Leck, 1975):

$$\mathrm{PDP}(\tau) = \frac{1}{N} \sum_{i=1}^{N} \left| h(\tau, t_i) \right|^2 \tag{10}$$

The resulting PDP can reduce the impact of noise. This is because the signal is coherent, and the noise is random, and for Gaussian white noise with a zero-average variance, the noise variance after the average period data is theoretically reduced, similar to the increment in the signal-to-noise ratio.

3.2 ROOT MEAN SQUARE DELAY SPREAD

Delay spread (DS) is another important channel constraint. There exists no general definition for the DS. Rigorously, it is the second central moment of PDP, but the explanation of mean/average time and the averaging aspect is very important for limited data archives of a non-stationary procedure. Because of its moment property and estimation from averaging, it is more vigorous to estimate the technique when associated to the power delay profile. In order to compare different multipath channels and summarize some common design principles of wireless systems, the methods of quantifying some parameters of multipath channels, RMS-DS is used, which can be calculated from PDP. The delay spread (DS) is normally the measure of multipath abundances of a communication channel. Moreover, it can be unstated as the difference among the time of arrival (TOA) of the first substantial multipath component (generally the LOS component) and the TOA of

*Corresponding author (A.Saleem, S.S.N. Yousaf). E-mail: asadalvi64@yahoo.com, shah.nisar@hotmail.com Transaction Journal of Engineering, Management, & Applied Sciences & Technologies. Volume 10 No.15 ISSN 2228-9860 eISSN 1906-9642 CODEN: ITJEA8 Paper ID:10A15A http://TUENGR.COM/V10A/10A15A.pdf DOI: 10.14456/ITJEMAST.2019.195

the last multipath component. DS is widely used in the characterization of a wireless channel, but it is also used for other multipath channels. Because it is a LOS channel, the first diameter (reference diameter) must be the PDP peak point, similar to the literature (Molisch, 2012). According to the sampling interval of the receiver to define the value of each sampling point as a valid diameter, the sampling point greater than the threshold value is considered as a valid diameter for the estimation of parameters. The time dispersion characteristics of broadband multipath channels are usually described quantitatively by average excess delay (ED) and RMS-DS. The average ED is a first-order moment for the power delay distribution, defined as (Molisch et al, 2012):

$$\bar{\tau} = \frac{\sum_k a_k^2 \tau_k}{\sum_k a_k^2} = \frac{\sum_k p(\tau_k)\tau_k}{\sum_k p(\tau_k)} \tag{11}$$

RMS-DS is basically the square root for second-order moments of PDP, defined as

$$\tau_{RMS} = \sqrt{\overline{\tau^2} - (\bar{\tau})^2} \tag{12}$$

whereas

$$\overline{\tau^2} = \frac{\sum_k a_k^2 \tau_k^2}{\sum_k a_k^2} = \frac{\sum_k p(\tau_k)\tau_k^2}{\sum_k p(\tau_k)} \tag{13}$$

The power $p(\tau_k)$ and delay τ_k are related to the diameter of the K-section respectively.

4. RESULTS AND DISCUSSIONS

For facilitating the complete understanding of this article, we insert the Nantong Tunnel environment for the SISO and MIMO channel measurement scheme of the two-dimensional plane map, respectively. The simulated campaign was accomplished in an empty subway tunnel at Zhongtian technology company (ZTT), Nantong, China, that is mostly functioned for a complete understanding of field realizations. This tunnel was basically 100m long and contains two parts: the initial part consists of arched tunnel with 50m length and the second part is rectangular tunnel of 50m length. The tunnel walls are protected with concrete material. We choose the rectangular-shaped tunnel for simulations. The cables are fixed along z-axis and beside tunnel walls, the elevation from the ground was considered along y-axis and the space between the Rx and the LCX was taken along$x$-axis. The total volume of rectangular shaped tunnel is specified as 50m (*length*) x 5m (*width*) x 3m (*height*). The dipole antenna was considered as a receiver antenna and *Wireless Insite* (*WISE*) software was used for measurements in the tunnel area. The WISE software is used to estimate both indoor and outdoor radio channel features by using the ray-tracing method. Moreover, it provides some antenna patterns such as Lambert's Law, half-wave dipole, isotropic and automatic (Fortune et al., 1995; Jimenez et al., 2017). The radiuses of outermost and innermost conductors of LCXs are given as 16mm and 6mm. The Nantong tunnel real-time inner view (Saleem et al., 2019) and WISE based tunnel construction are shown in Figure.2 and the configurations of static parameters are given in Table.1. Loc1, Loc2, and Loc3 are three different

positions of LCXs at 2.7m, 1.9m and 1.15m high from the ground level.

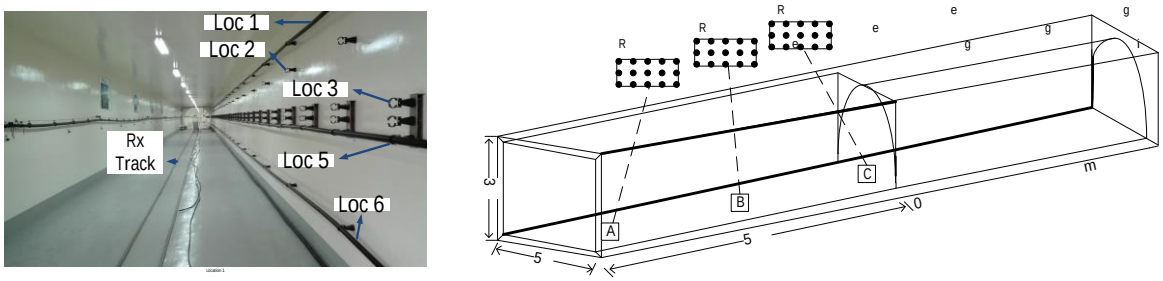

(a) (b)

Figure 2: (a) The real-time Nantong tunnel inner view, (b) the tunnel construction in Wireless Insite.

For SISO and MIMO channel measurement scheme of PDP in the Nantong tunnel for the two-dimensional plane map are given in Figure 3 (a) and (b). When the SISO channel is measured, the LCX is placed 2.7m high from the ground of tunnel along z-axis, and the receiver is measured at 2m away from the distance of the LCX along x-axis. In SISO system, we divided it into three regions as Region1, Region2, and Region3, respectively; whereas each region has three rows of receiving antennas and each row have 25 locations of receiving antennas. So, in each region, we have 75 receiving antennas and each row is apart 0.5m distance from others. Also, in each row, the distance between two consecutive antennas is 0.5 λ and the slot period of LCX was considered as 0.6m. Region1 contains from 0m to 2m, Region2 contains from 24m to 26m and Region3 contains from 48m to 50m in rectangular Nantong tunnel. For the MIMO system, the first LCX working as Tx-1 is at 2.7m high from ground and second LCX working as Tx-2 is 1.9m high from ground.

Table 1: The Measuring Parameters.

Unit	Parameter
Carrier Frequency	1.8GHz
Transmitted Power	20dBm
Bandwidth	40.8MHz
Tx-Antenna	ZTT-LCX of 50m length
Rx-Antenna	UHA9125D Dipole Antenna
Antenna Gain	2.15 dBi
Height of LCX at Loc 1	2.7m
Height of LCX at Loc 3	1.9m
Height of LCX at Loc 5	1.5m
Height of Rx-Antenna	1.6m
LCX spacing	Loc 1 and Loc 3, 0.8m
LCX spacing	Loc 1 and Loc 5, 1.2m
LCX spacing	Loc 3 and Loc 5, 0.4m
Slots period of LCX	0.6m
Sampling Rate	81.6MHz
Resistance	50ohm
Measurement Time	50ms

Moreover, we considered three receiving antennas arrays as Rx-1, Rx2 and Rx-3 at 0m, 24m, 48m distances away from start of tunnel, respectively. Each receiver consists of 75 virtual receiving antenna arrays, whereas distance between two consecutive receiver antenna arrays is 0.5 λ.

*Corresponding author (A.Saleem, S.S.N. Yousaf). E-mail: asadalvi64@yahoo.com, shah.nisar@hotmail.com

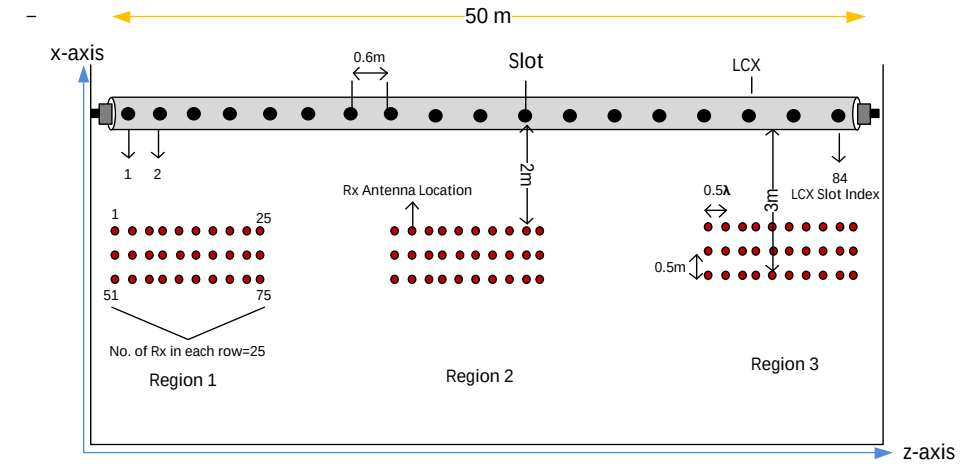

(a)

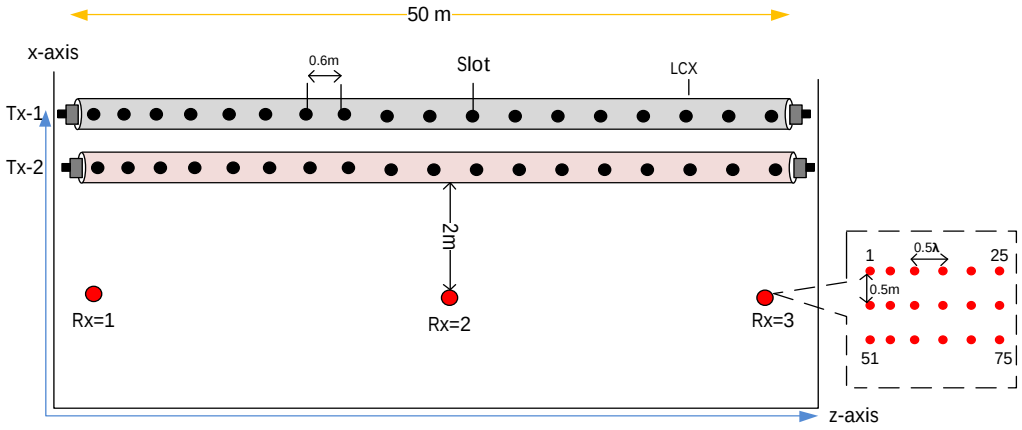

(b)

Figure 3: The transmitting and receiving antenna locations
(a) for the SISO system, (b) for the MIMO system.

In this paper, 2,150 cycles of channel impact response, that is, N=2150, are measured. By averaging the data of 2150 frames, the PDP of each sub-channel is obtained, and Figure 4 shows the PDP's comparison of Rx antennas with the horizontal and vertical polarized LCX slots in Region1. In each region, there are 3 arrays of Rx antennas and each array contains 25 Rx antennas, whereas the period of LCX slots is 0.6m for 50m long LCX. In comparison, we have found that horizontal polarized LCX has superior performance for PDP than the vertical polarized LCX by using (10). The first array of slots has higher received power between Tx and Rx than other arrays due to less distance as can be seen in Figure 4. It is clear the first array in each region has improved PDP than the other two arrays of receiving antennas.

Similarly, we considered the other two regions (Region2 and Region3) for PDP's comparison for both vertical and horizontal polarized LCX slots in Figure 5 and Figure 6, respectively and we have found that Region1 has relatively strongest power than others and horizontal polarized LCX performs superior to vertical polarized LCX for the SISO system.

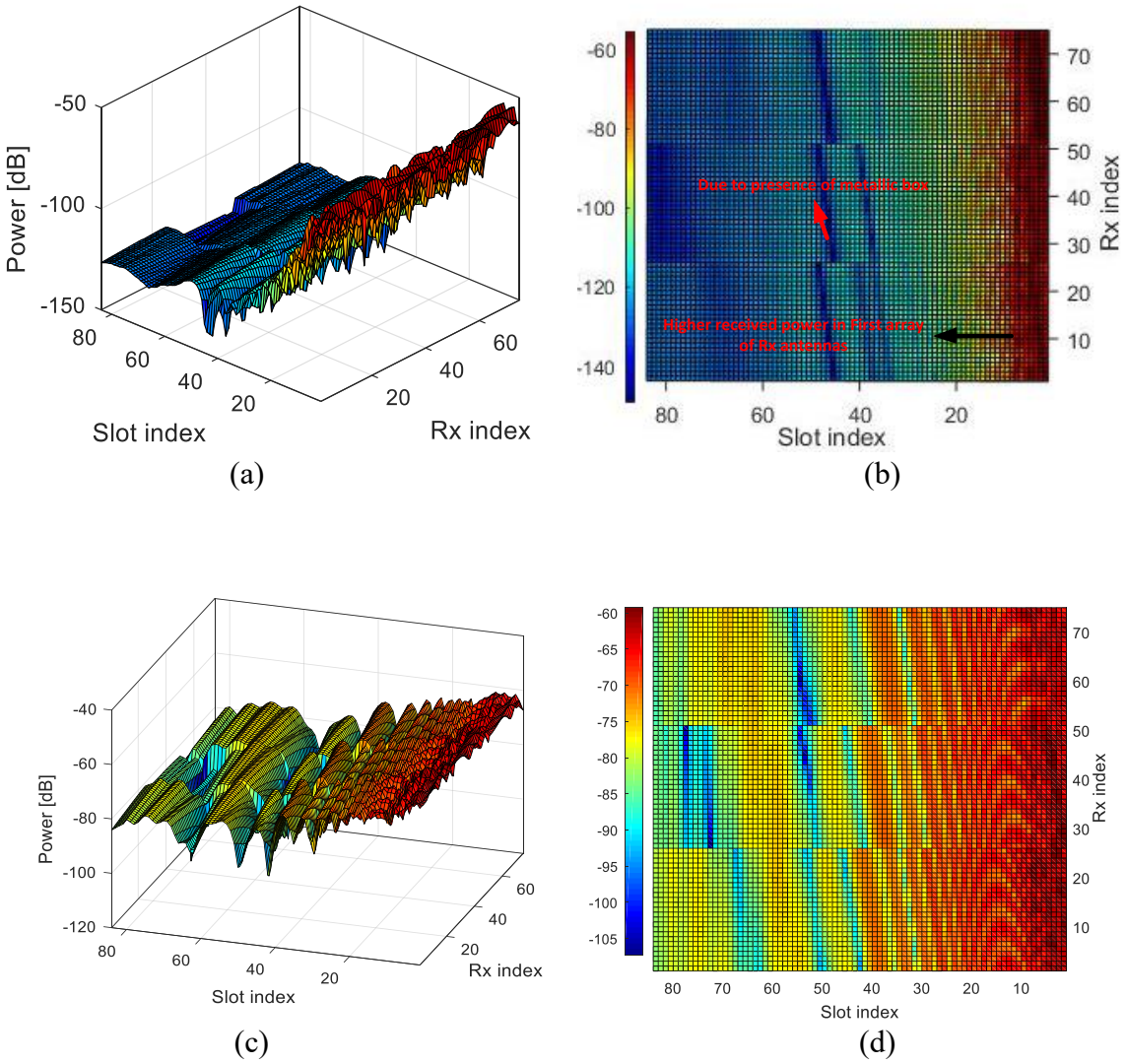

Figure 4: The PDP comparison for the SISO system of 75 Rx antennas in Region1 for Horizontally polarized LCX slots (a) 3D side view of PDP, (b) 2D upper view of PDP. The PDP comparison in Region1 for Vertically polarized LCX slots (c) 3D side view of PDP, (d) 2D upper view of PDP.

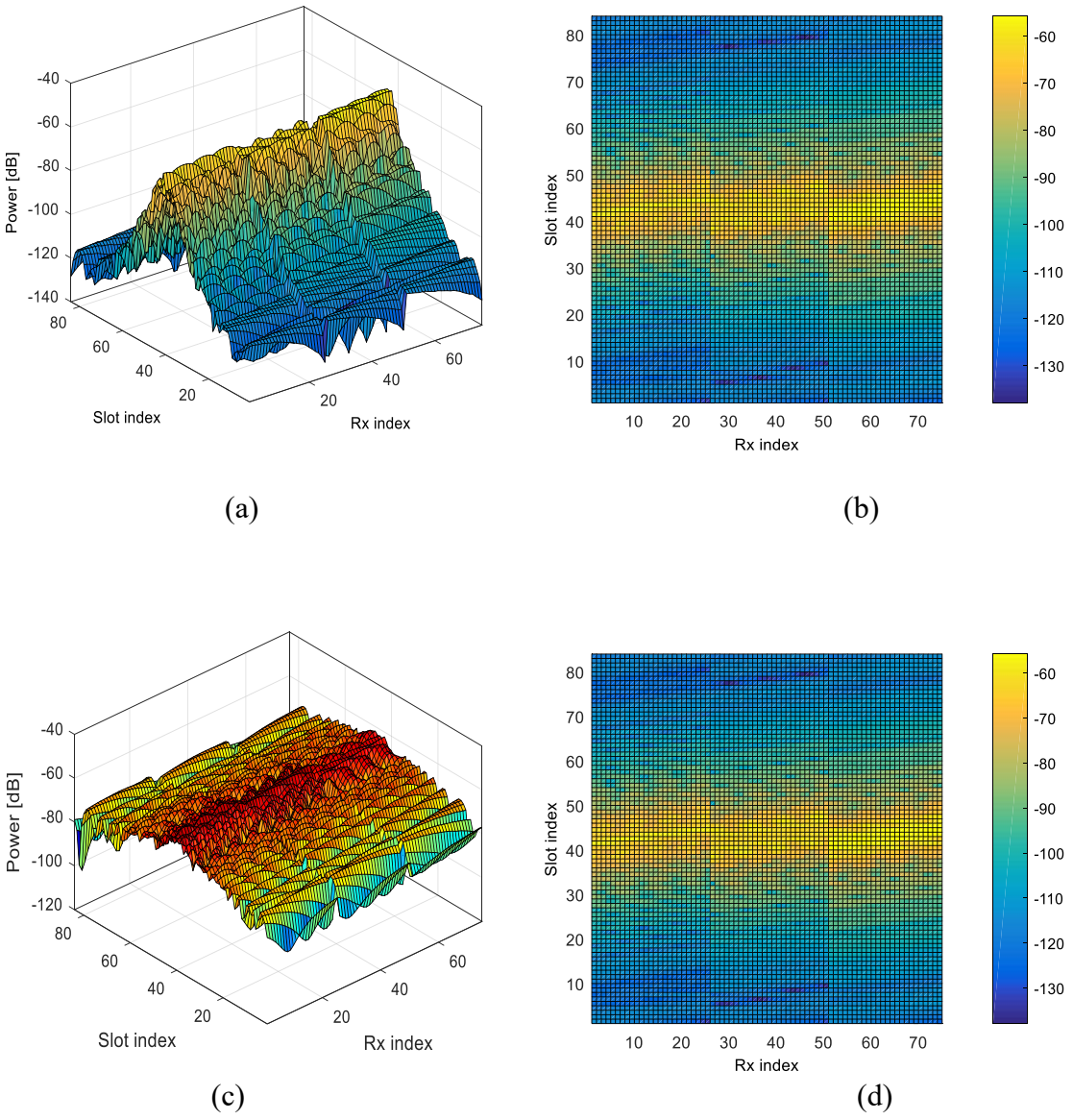

Figure 5: The PDP comparison for SISO system of 75 Rx antennas in Region2 for Horizontal polarized LCX slots (a) 3D side view of PDP, (b) 2D upper view of PDP. The PDP comparison in Region2 for Vertical polarized LCX slots (c) 3D side view of PDP, (d) 2D upper view of PDP.

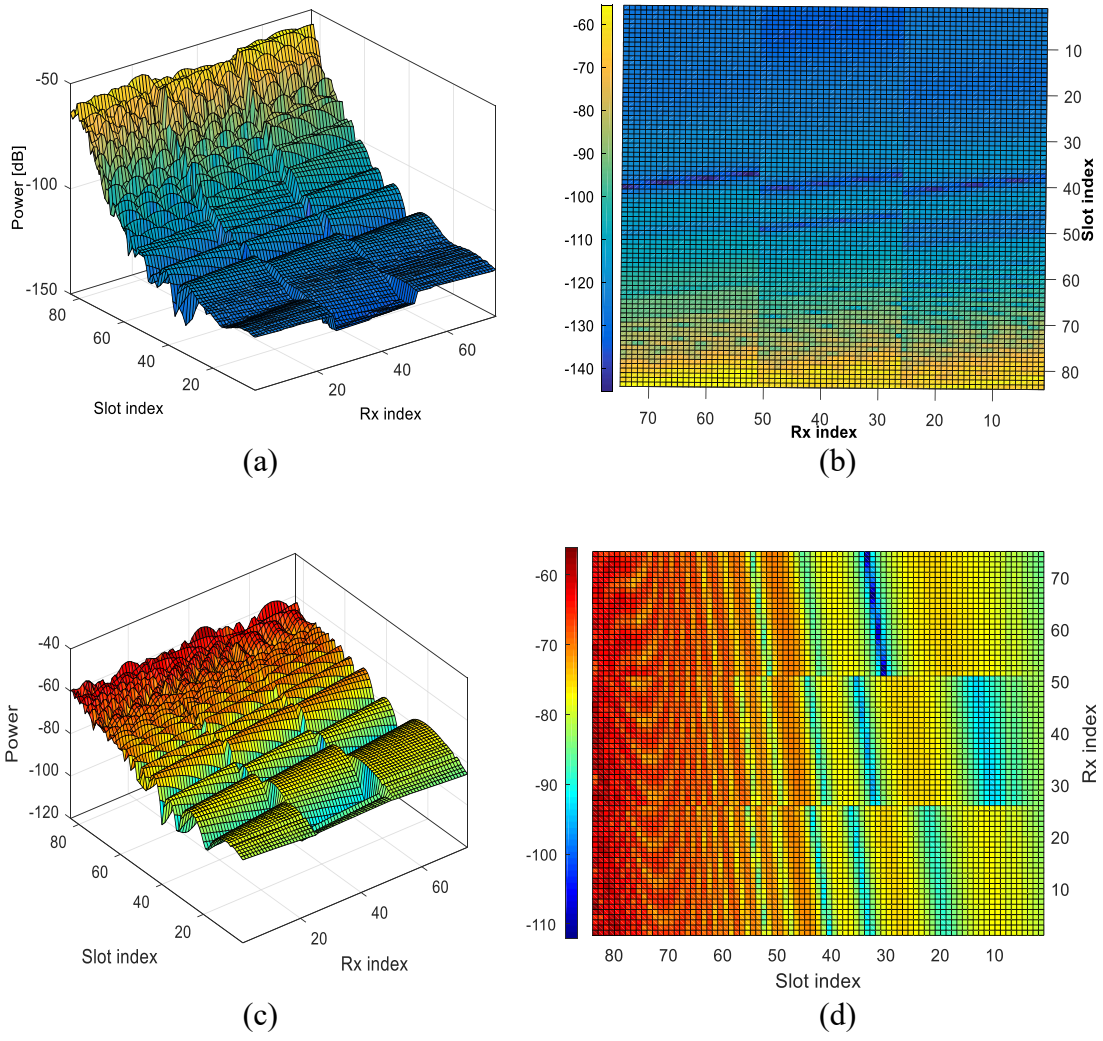

Figure 6: The PDP comparison for SISO system of 75 Rx antennas in Region3 for Horizontal polarized LCX slots (a) 3D side view of PDP, (b) 2D upper view of PDP. The PDP comparison in Region3 for Vertical polarized LCX slots (c) 3D side view of PDP, (d) 2D upper view of PDP.

Due to the presence of a single metal box in the mid rectangular shaped tunnel which originates many reflections, moreover, the junction of rectangular and arched tunnel has extra concrete wall material which also causes extra reflections. So, due to these reasons, Region1 has higher performance as compared to other two regions (Region 2 and Region 3).

For further investigation of PDP, we evaluated the PDP of the MIMO system for the different receivers as shown in Figure 3 (b). We considered the 2x3 MIMO system by using virtual receiving antenna arrays. The two different LCXs of 50m long at 2.7m and 1.9m high from the ground were examined. We took 3 receivers as Rx-1, Rx-2, and Rx-3, whereas each receiver has virtual array of 75 receiving antennas with 0.5 λ spacing. So, totally we will have 450 virtual Rx's for 2x3 MIMO systems. The PDP relation of MIMO system corresponding different numbers of Rx for horizontal and vertical polarized LCX's is given in Figure 7.

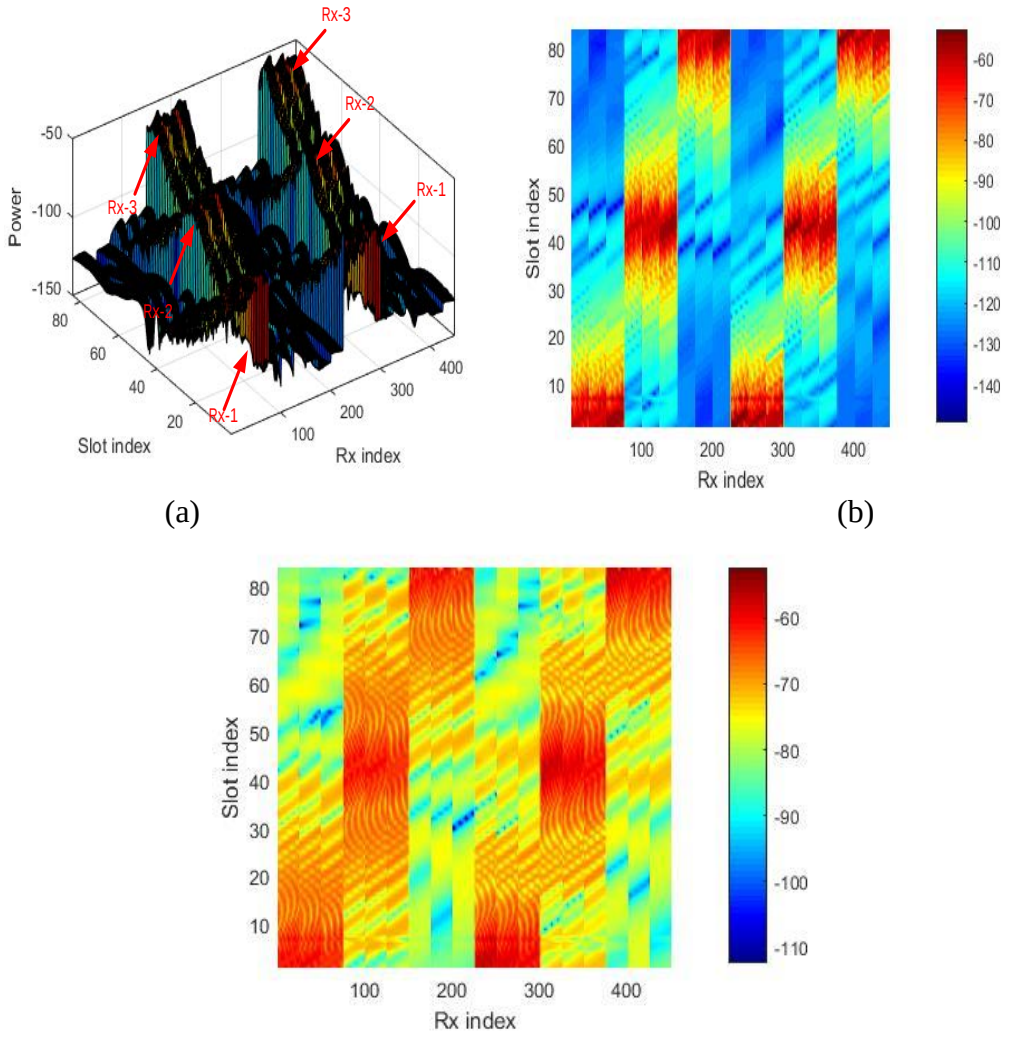

Figure 7: The PDP comparison for the MIMO system of virtual 450 Rx antennas for (a)Horizontal polarized LCX's slots in 3D side view (b) 2D upper view of PDP for horizontal polarized LCX's (c) 2D upper view of PDP for vertical polarized LCX's.

According to the formula of RMS-DS, the statistical parameters of average RMS-DS measured for the SISO channel with horizontally polarized configurations of LCX at 2.7m high from ground level according to Figure 3 (a) where receiving points scenario is calculated for all three regions in Figure 8. It can be seen that Region1 has a higher value of RMS-DS as compared to other two regions. Due to presence of metallic box in Region2 and extra concrete wall portion in Region3, there exists a more number of reflections, so Region1 have better performance in terms of PDP and RMS-DS than other regions.

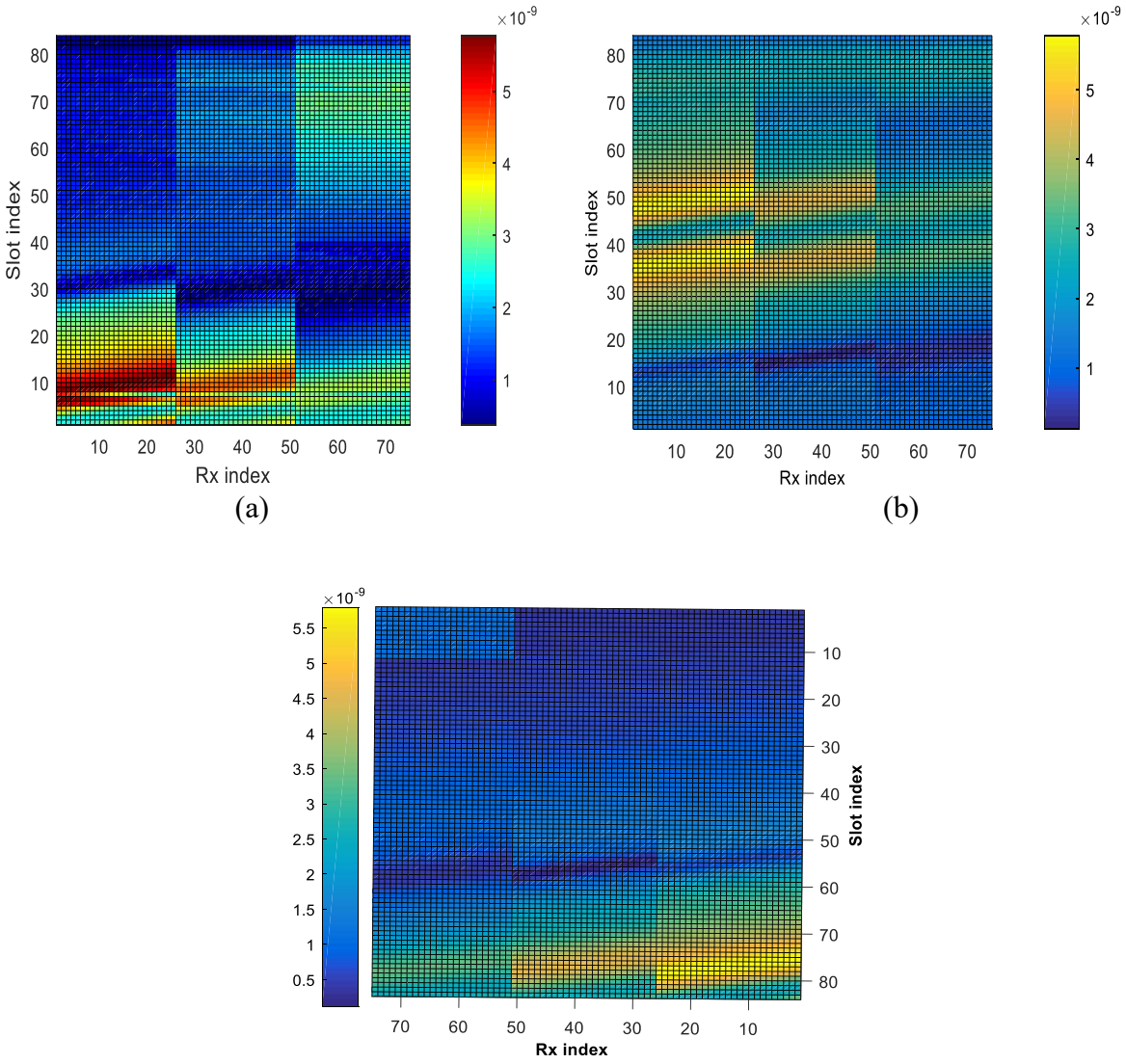

Figure 8: The RMS-DS comparison for SISO system for Horizontal polarized LCX (84 slots) at 2.7m high with receiving antenna in Region1 (a), In Region2 (b) In Region3 (c).

5. CONCLUSION

In this paper, we considered the simulated campaign for SISO and MIMO systems in the tunnel environment at 1.8GHz frequency band for both horizontal and vertical polarized LCXs. We have found the response of PDP and RMS-DS over different locations of LCXs and the receiving antennas. We have proved that horizontal polarized LCXs have superior performance than the vertical polarized LCXs when considered the SISO and MIMO systems individually. Furthermore, we have proved that Region1 has improved PDP and RMS-DS values than the other two regions (Region2 and Region3) in tunnel environment and the first array of receiving antennas which are a minimum distance from LCX, has better PDP and RMS-DS than the other two Rx antennas arrays. As a result, this study delivers a proficient knowledge for optimal model designing and moreover, it offers improved platform for the LTE-M system by deploying the LCX in the tunnel.

*Corresponding author (A.Saleem, S.S.N. Yousaf). E-mail: asadalvi64@yahoo.com, shah.nisar@hotmail.com Volume 10 No.15 ISSN 2228-9860 eISSN 1906-9642 CODEN: ITJEA8 Paper ID:10A15A http://TUENGR.COM/V10A/10A15A.pdf DOI: 10.14456/ITJEMAST.2019.195

6. AVAILABILITY OF DATA AND MATERIAL

The used or generated data in this study is available by request to the corresponding author.

7. REFERENCES

Nakamura, N., H. Tsunomachi, and R. Fukui, “Road vehicle communication system for vehicle control using leaky coaxial cable,” IEEE Communications Magazine, vol. 34, no. 10, pp. 84–89, 1996.

Schwarz, S. and M. Rupp, “Society in motion: challenges for LTE and beyond mobile communications,” IEEE Communications Magazine, vol. 54, no. 5, pp. 76–83, 2016.

Li, D. and J. Wang, “Effect of antenna parameters on the field coverage in tunnel environments,” International Journal of Antennas and Propagation, vol. 2016, Article ID 8180124, 10 pages, 2016.

Wang, H., F. R. Yu, and H. Jiang, “Modeling of radio channels with leaky coaxial cable for LTE-M based CBTC systems,” IEEE Communications Letters, vol. 20, no. 5, pp. 1038– 1041, 2016.

Wang, X., J. Wang, Z. Zhang, and M. Chen, “Coupling characteristics between leaky coaxial cables with and without obstacle,” in 2012 10th International Symposium on Antennas, Propagation & EM Theory (ISAPE2012), pp. 612–615, Xian, China, 2012.

Zhao, Z., X. Yang, and S. Guo, “A coupling loss algorithm of leaky coaxial cable in the blind zone”, Mechatronic and Automation ICMA, International Conference on. IEEE, pp. 919-923, 2008.

Fuschini, F., E. M. Vitucci, G. Falciasecca, and V. Degli-Esposti, “Ray tracing propagation modeling for future small-cell and indoor applications: A review of current techniques”, Radio Science, vol. 50, no. 6, pp. 469-485, 2015.

Kim, D. H., and H. J. Eom, "Radiation of a leaky coaxial cable with narrow transverse slots", IEEE transactions on antennas and propagation vol. 55, no. 1, pp. 107-110, 2007.

Forooshani, A. Emami, C. Y. T. Lee, and D. G. Michelson. "Effect of antenna configuration on MIMO-based access points in a short tunnel with infrastructure", IEEE Transactions on Communications, vol. 64, no. 5, pp. 1942-1951, 2016.

Medbo, J., and A. Nilsson. “Leaky coaxial cable MIMO performance in an indoor office environment”, In Personal Indoor and Mobile Radio Communications (PIMRC), 2012 IEEE 23rd International Symposium on, pp. 2061-2066, 2012.

He, Ruisi, Zhangdui Zhong, and Cesar Briso. "Broadband channel long delay cluster measurements and analysis at 2.4 GHz in subway tunnels." In 2011 IEEE 73rd Vehicular Technology Conference (VTC Spring), pp. 1-5, 2011.

Li, Shuang-de, Yuan-Jian Liu, Le-ke Lin, Zhong Sheng, Xiang-Chen Sun, Zhi-peng Chen, and Xiao-jun Zhang. "Channel measurements and modeling at 6 GHz in the tunnel environments for 5G wireless systems." International Journal of Antennas and Propagation 2017.

Collonge, Sylvain, Gheorghe Zaharia, and Ghaïs El Zein. "Influence of the furniture on 60 GHz radio propagation in a residential environment." In Signals, Circuits and Systems, 2003. SCS 2003. International Symposium on, vol. 2, pp. 413-416, 2003.

Liao, Shu-Han, Chien-Ching Chiu, Chien-Hung Chen, and Min-Hui Ho. "Channel characteristics of MIMO–WLAN communications at 60 GHz for various corridors." EURASIP Journal on Wireless Communications and Networking, vol. 96, no. 1, 2013.

Zhang, X., X. Yang, L. Guo, Z. Zhao, Research on the radiated field's distribution of leaky coaxial cable in the blind zone, 2006 1st International Symposium on Systems and Control in Aerospace and Astronautics, IEEE, pp. 4-7, 2006.

Fontan, F. P., and P. M. Espieira, Modelling the Wireless Propagation Channel: A simulation approach with Matlab: WILEY, 2008.

Molisch, A. F., Wireless Communications. West Sussex, England: Wiley, 2011.T. Cui, and C. Tellambura, "Power delay profile and noise variance estimation for OFDM," Communications Letters, IEEE, vol. 10, no. 1, pp. 25-27, 2006.

Cui, T. and C. Tellambura, "Power delay profile and noise variance estimation for ofdm," Communications Letters, IEEE, vol. 10, no. 1, pp. 25-27, 2006.

Cui, Tao, and Chintha Tellambura. "Cyclic-prefix based noise variance and power delay profile estimation for OFDM systems." In PACRIM. 2005 IEEE Pacific Rim Conference on Communications, Computers and Signal Processing, 2005., pp. 518-521, 2005.

Cox, D C, R Leck. Distributions of multipath delay spread and average excess delay for 910-MHz urban mobile radio paths [J]. Antennas and Propagation, IEEE Transactions on, vol. 23, no. 2, pp. 206-213, 1975.

Molisch, A F. Wireless communications [M]. John Wiley & Sons, 2012.

Fortune, S. J., D. M. Gay, B. W. Kernighan, O. Landron, R. A. Valenzuela, and M. H. Wright, "WISE design of indoor wireless systems: practical computation and optimization," IEEE Computational Science and Engineering, vol. 2, no. 1, pp. 58–68, 1995.

Jimenez, M. J. C., K. Arana, and M. R. Arias, "Outdoor-to-indoor propagation mechanisms in multistorey building for 0.85 GHz and 1.9 GHz bands," in 2017 IEEE 37th Central America and Panama Convention (CONCAPAN XXXVII), pp. 1–6, Managua, Nicaragua, 2017.

Saleem, Asad, Min Wang, Guoxin Zheng, and Xiaoyu Yin. "Spatial Characteristics of Wideband Channels Using Leaky Coaxial Cables in Tunnel Scenario." International Journal of Antennas and Propagation 2019.

Dr.Asad Saleem has received his PhD degree from School of Communication and Information Engineering, Shanghai University, Shanghai, China. He has completed his Master's degree from Quaid-iAzam University, Islamabad, Pakistan. His research interests are Massive MIMO systems, wireless ad hoc networks, mmWAVE channel, and antenna designing.

Sherazi Syed Nisar Yousaf is a Master's degree student at School of Communication and Information Engineering, Taiyuan University of Technology, China. His research interests are in the areas of statistical signal processing and wireless communications.